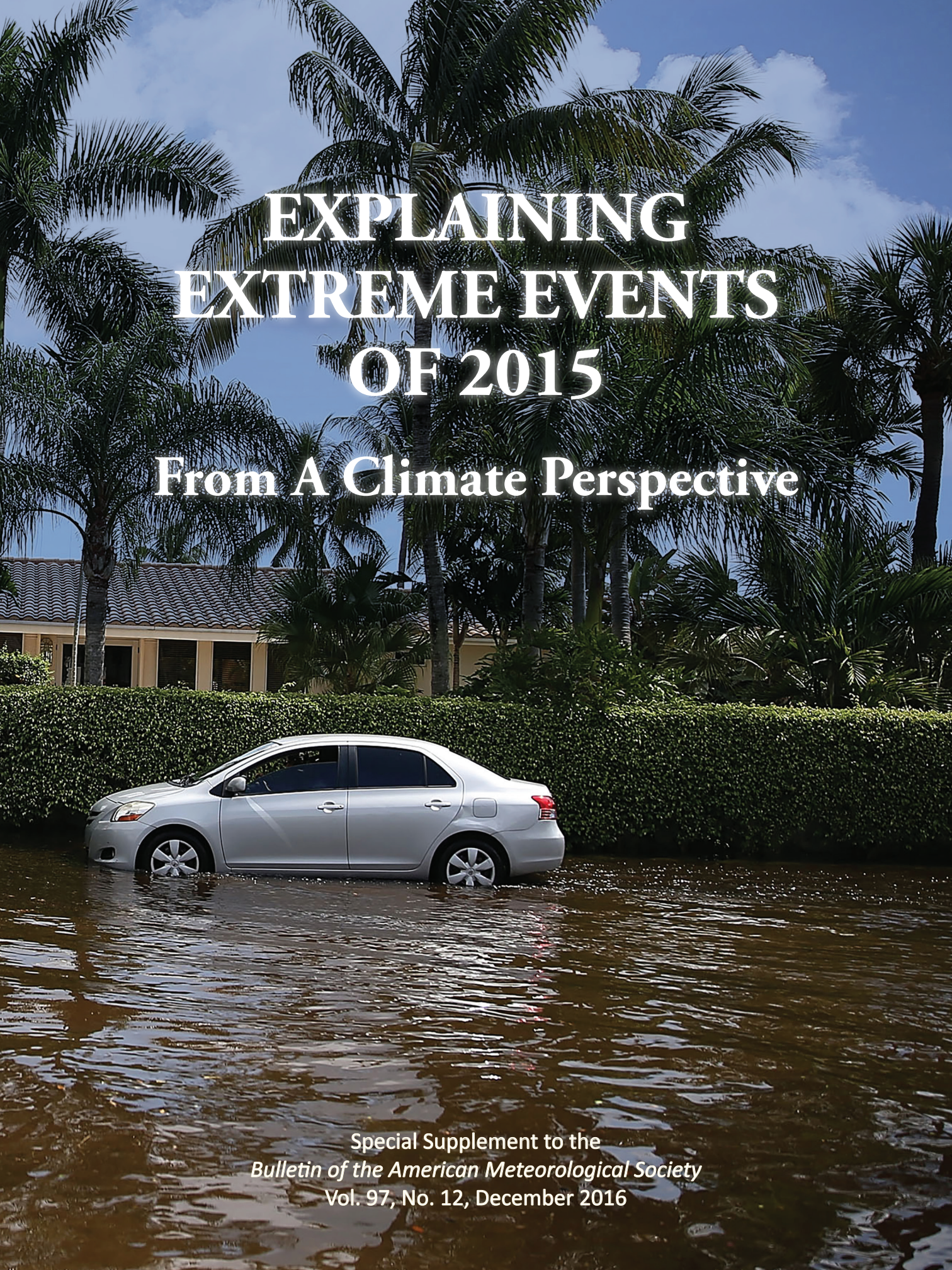

EXPLAINING EXTREME EVENTS OF 2015

From A Climate Perspective

Special Supplement to the
Bulletin of the American Meteorological Society
Vol. 97, No. 12, December 2016

EXPLAINING EXTREME EVENTS OF 2015 FROM A CLIMATE PERSPECTIVE

Editors

Stephanie C. Herring, Andrew Hoell, Martin P. Hoerling, James P. Kossin,
Carl J. Schreck III, and Peter A. Stott

Special Supplement to the

Bulletin of the American Meteorological Society

Vol. 97, No. 12, December 2016

American Meteorological Society

Corresponding Editor:

Stephanie C. Herring, PhD
NOAA National Centers for Environmental Information
325 Broadway, E/CC23, Rm 1B-131
Boulder, CO, 80305-3328
E-mail: stephanie.herring@noaa.gov

Cover Credit:

©Photo by Joe Raedle/Getty Images—A vehicle drives through flooded streets caused by a combination of the lunar orbit which caused seasonal high tides and what many believe is the rising sea levels due to climate change on September 30, 2015, in Fort Lauderdale, Florida. South Florida is projected to continue to feel the effects of climate change, and many of the cities have begun programs such as installing pumps or building up sea walls to try and combat the rising oceans.

HOW TO CITE THIS DOCUMENT

Citing the complete report:

Herring, S. C., A. Hoell, M. P. Hoerling, J. P. Kossin, C. J. Schreck III, and P. A. Stott, Eds., 2016: Explaining Extreme Events of 2015 from a Climate Perspective. *Bull. Amer. Meteor. Soc.*, **97 (12)**, S1–S145.

Citing a section (example):

Partain, J. L., and Coauthors, 2016: An assessment of the role of anthropogenic climate change in the Alaska fire season of 2015 [in "Explaining Extremes of 2015 from a Climate Perspective"]. *Bull. Amer. Meteor. Soc.*, **97 (12)**, S14–S18, doi:10.1175/BAMS-D-16-0149.

EDITORIAL AND PRODUCTION TEAM

Riddle, Deborah B., Lead Graphics Production, NOAA/NESDIS National Centers for Environmental Information, Asheville, NC

Veasey, Sara W., Visual Communications Team Lead, NOAA/NESDIS National Centers for Environmental Information, Asheville, NC

Love-Brotak, S. Elizabeth, Graphics Support, NOAA/NESDIS National Centers for Environmental Information, Asheville, NC

Fulford, Jennifer, Editorial Support, Telesolv Consulting LLC, NOAA/NESDIS National Centers for Environmental Information, Asheville, NC

Griffin, Jessicca, Graphics Support, Cooperative Institute for Climate and Satellites-NC, North Carolina State University, Asheville, NC

Maycock, Tom, Editorial Support, Cooperative Institute for Climate and Satellites-NC, North Carolina State University, Asheville, NC

Misch, Deborah J., Graphics Support, Telesolv Consulting LLC, NOAA/NESDIS National Centers for Environmental Information, Asheville, NC

Osborne, Susan, Editorial Support, Telesolv Consulting LLC, NOAA/NESDIS National Centers for Environmental Information, Asheville, NC

Sprain, Mara, Editorial Support, LAC Group, NOAA/NESDIS National Centers for Environmental Information, Asheville, NC

Young, Teresa, Graphics Support, STG, Inc., NOAA/NESDIS National Centers for Environmental Information, Asheville, NC

TABLE OF CONTENTS

ABSTRACT—Stephanie C. Herring, Andrew Hoell, Martin P. Hoerling, James P. Kossin, Carl J. Schreck III, and Peter A. Stott

This fifth edition of explaining extreme events of the previous year (2015) from a climate perspective continues to provide evidence that climate change is altering some extreme event risk. Without exception, all the heat-related events studied in this year's report were found to have been made more intense or likely due to human-induced climate change, and this was discernible even for those events strongly influenced by the 2015 El Niño. Furthermore, many papers in this year's report demonstrate that attribution science is capable of separating the effects of natural drivers including the strong 2015 El Niño from the influences of long-term human-induced climate change.

Other event types investigated include cold winters, tropical cyclone activity, extreme sunshine in the United Kingdom, tidal flooding, precipitation, drought, reduced snowpack in the U.S. mountain west, arctic sea ice extent, and wildfires in Alaska. Two studies investigated extreme cold waves and monthly-mean cold conditions over eastern North America during 2015, and find these not to have been symptomatic of human-induced climate change. Instead, they find the cold conditions were caused primarily by internally generated natural variability. One of these studies shows winters are becoming warmer, less variable, with no increase in daily temperature extremes over the eastern United States. Tropical cyclone activity was extreme in 2015 in the western North Pacific (WNP) as measured by accumulated cyclone energy (ACE). In this report, a study finds that human-caused climate change largely increased the odds of this extreme cyclone activity season. The 2015 Alaska fire season burned the second largest number of acres since records began in 1940. Investigators find that human-induced climate change has increased the likelihood of a fire season of this severity.

Confidence in results and ability to quickly do an attribution analysis depend on the "three pillars" of event attribution: the quality of the observational record, the ability of models to simulate the event, and our understanding of the physical processes that drive the event and how they are being impacted by climate change. A result that does not find a role for climate change may be because one or more of these three elements is insufficient to draw a clear conclusion. As these pillars are strengthened for different event types, confidence in the presence and absence of a climate change influence will increase.

This year researchers also link how changes in extreme event risk impact human health and discomfort during heat waves, specifically by looking at the role of climate change on the wet bulb globe temperature during a deadly heat wave in Egypt. This report reflects a growing interest within the attribution community to connect attribution science to societal impacts to inform risk management through "impact attribution." Many will watch with great interest as this area of research evolves in the coming years.

15. ASSESSING THE CONTRIBUTIONS OF LOCAL AND EAST PACIFIC WARMING TO THE 2015 DROUGHTS IN ETHIOPIA AND SOUTHERN AFRICA

Chris Funk, Laura Harrison, Shraddhanand Shukla, Andrew Hoell, Diriba Korecha, Tamuka Magadzire, Gregory Husak, and Gideon Galu

Anthropogenic warming contributed to the 2015 Ethiopian and southern African droughts by increasing El Niño SSTs and local air temperatures, causing reduced rainfall and runoff, and contributing to severe food insecurity.

Introduction. In northern Ethiopia (7°–14°N, 36.5°–40.5°E, NE) during June–September (JJAS) of 2015 and in southern Africa (13.5°–27°S, 26.5°–36°E, SA) during December–February (DJF) of 2015/16, main growing seasons rains were extremely poor. In Ethiopia, Climate Hazards Group Infrared Precipitation with Stations (CHIRPS) (Funk et al. 2015c) and Centennial Trends (Funk et al. 2015b) data indicated one of the worst droughts in more than 50 years (FEWSNET 2015). More than ten million people currently require humanitarian relief (FEWSNET 2016a). SA rains were also extremely poor (FEWSNET 2016b); in Mozambique and Malawi, February maize prices were more than twice the five-year average, and in Zimbabwe the president has declared a national disaster in view of the El Niño–induced poor rains and the escalating food insecurity situation.

NE has been experiencing long-term rainfall declines (Funk et al. 2008; Funk et al. 2005; Jury and Funk 2013; Viste et al. 2012; Williams et al. 2012). The eastern Ethiopian highlands have exhibited recurrent soil moisture and runoff deficits since the 1990s (Funk et al. 2015c). NE rains in 2015 were the driest on record, but station data density prior to 1950 is very sparse for Ethiopia (Funk et al. 2015b). SA rainfall does not exhibit a decline, but the 2015–16 drought was severe. The impact of ENSO on Ethiopian rainfall is well documented (Fig. S15.1; Camberlin 1997; Degefu 1987; Diro et al. 2011; Gissila et al. 2004; Korecha and Barnston 2007; Korecha and Sorteberg 2013; Segele and Lamb 2005): the warm phase of ENSO is associated with suppressed rains during the main wet season (JJAS) over north and central Ethiopia. There have also been numerous papers documenting a negative teleconnection between El Niño and SA rainfall (Supplemental Fig. S15.1; Hoell et al. 2015; Jury et al. 1994; Lindesay 1988; Misra 2003; Nicholson and Entekhabi 1986; Nicholson and Kim 1997; Reason et al. 2000; Rocha and Simmonds 1997).

Is Anthropogenic Climate Change Causing More Extreme El Niños? Our attribution approach is similar to our 2014 study (Funk et al. 2015a) examining boreal spring rainfall deficits in Kenya and southeastern Ethiopia. We first assess changes in Niño-3.4 SST extremes based on climate change simulations and then interpret these results using empirical relationships between Niño-3.4 SSTs and regional rainfall and air temperatures. Figures 15.1a,b examine JJAS and DJF Niño-3.4 SSTs (Huang et al. 2015) from observations (blue/red bars) and a multimodel climate change ensemble (red lines and blue shading; SST simulations from 19 model combinations and 34 simulations; 2006–15 simulation values were based on the RCP8.5 experiment; for details see https://climexp.knmi.nl) based on simulations from 1861 through 2100. For each of the 34 simulations, for each year, the top six Niño-3.4 SST events from the surrounding 30 years typified El Niño. The heavy red lines depict the ensemble average of these values for each year. The thin red lines identify the 80% confidence interval associated with the ensemble spread. The climate change distribution agrees reasonably well with the observed increasing strength of moderate-strong Niño-3.4 events. The simulations predict increasingly extreme Niño-3.4 events, and

AFFILIATIONS: Funk—U.S. Geological Survey and University of California Santa Barbara, Santa Barbara, California; Harrison, Shukla, Korecha, Magadzire, Husak, and Galu—University of California Santa Barbara, Santa Barbara, California; Hoell—NOAA/Earth System Research Laboratory Physical Sciences Division, Boulder, Colorado

DOI:10.1175/BAMS-D-16-0167.1

A supplement to this article is available online (10.1175/BAMS-D-16-0167.2)

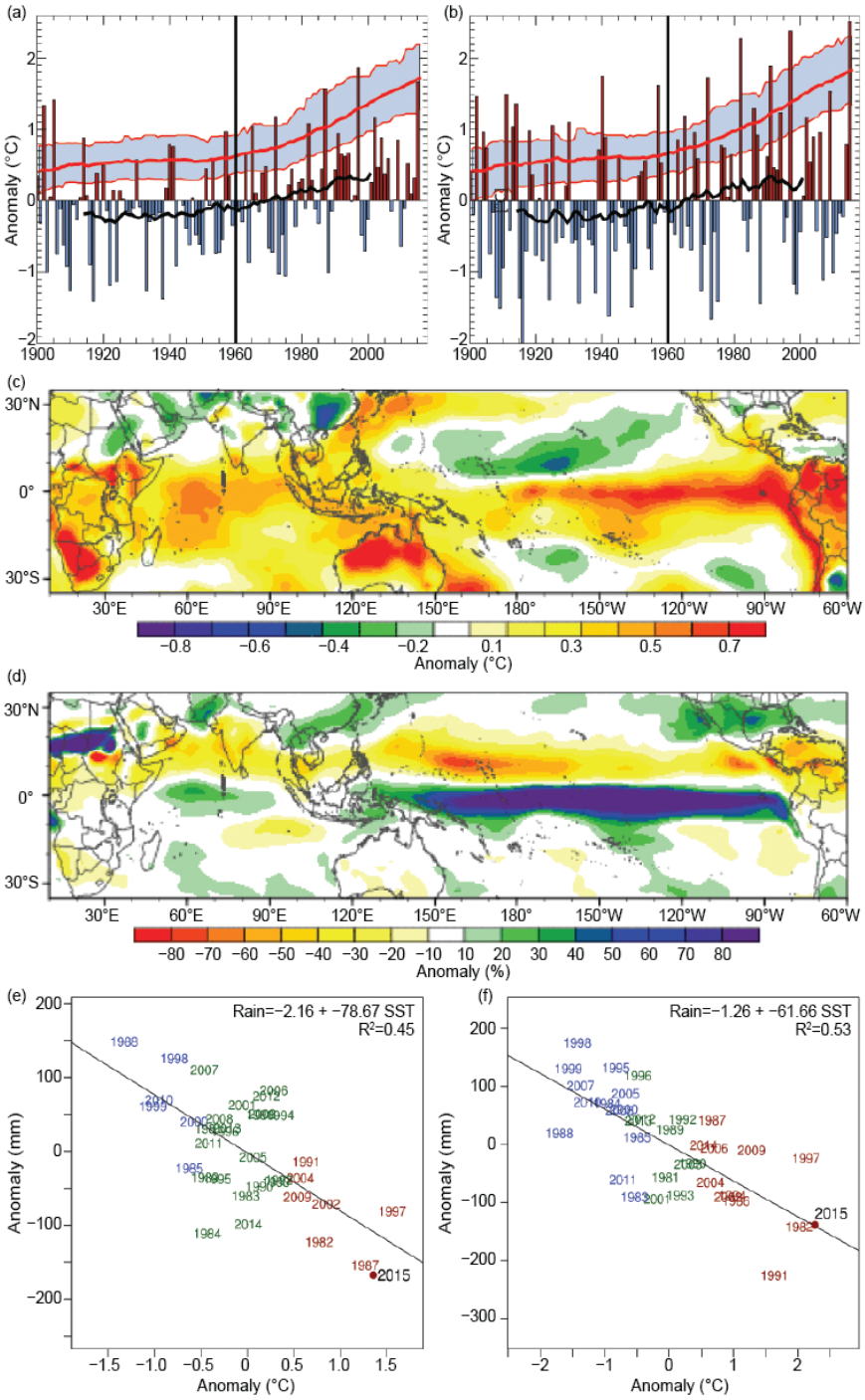

Fig. 15.1. (a),(b) Observed Niño-3.4 SST anomalies (bars) along with associated 30-yr means (thick black line). SST simulations are from 19 model combinations and 34 simulations; 2006–15 simulation values were based on the RCP8.5 experiment (for details see https://climexp.knmi.nl). Thick and thin red lines show running 30-yr climate change ensemble El Niño SSTs (see www.esrl.noaa.gov/psd/repository/alias/facts). (c),(d) Changes in the DJF Geophysical Fluid Dynamics Laboratory Atmospheric Model version 3 near-surface air temperatures and precipitation during 1980–2015 El Niño events versus 1920–79 El Niño events. Results based on the 17-member ensemble mean. (e),(f) Scatterplots between Niño-3.4 SST and observed NE and SA rainfall anomalies.

this is what we see in the SST observations (Supplemental Figs. S15.1a,b): increasingly intense El Niño events.

To estimate radiatively forced changes in ENSO maxima, we subtracted the average 1946–75 ensemble sea surface temperatures over the Niño-3.4 region (temporal center point marked with the black vertical lines in Figs. 15.1a,b) from the 2000–29 Niño-3.4 values (the last point on the thick red line). For DJF and JJAS, this gives us an estimated change of +1.2°C. Using the 80% confidence intervals for 2015–16 and repeating this calculation lets us establish a range of values $\Delta T_{DJF} = +1.2° \pm 0.5°C$ and $\Delta T_{JJAS} = +1.1° \pm 0.5°C$.

We next examine three atmospheric GCM simulation ensembles, drawn from the Earth Systems Research Laboratory Facility for Climate Assessments (FACTS; see www.esrl.noaa.gov/psd/repository/alias/facts). Using FACTS, we examined differences between 1980–2015 and 1920–79 moderate-to-strong El Niños, using atmospheric General Circulation Model (AGCM) simulations. Figures 15.1c,d show results for a single model for DJF. Supplemental Fig. S15.2 shows similar results for all three models for both seasons. Over the tropical Pacific and Indian Oceans (Fig. 15.1c), recent El Niños have been associated with much warmer conditions (> +0.8°C), consistent with Figs. 15.1a,b, but have also been potentially influenced by natural decadal variability (Wittenberg 2009).

Accompanying the warming is a very large (70%+)

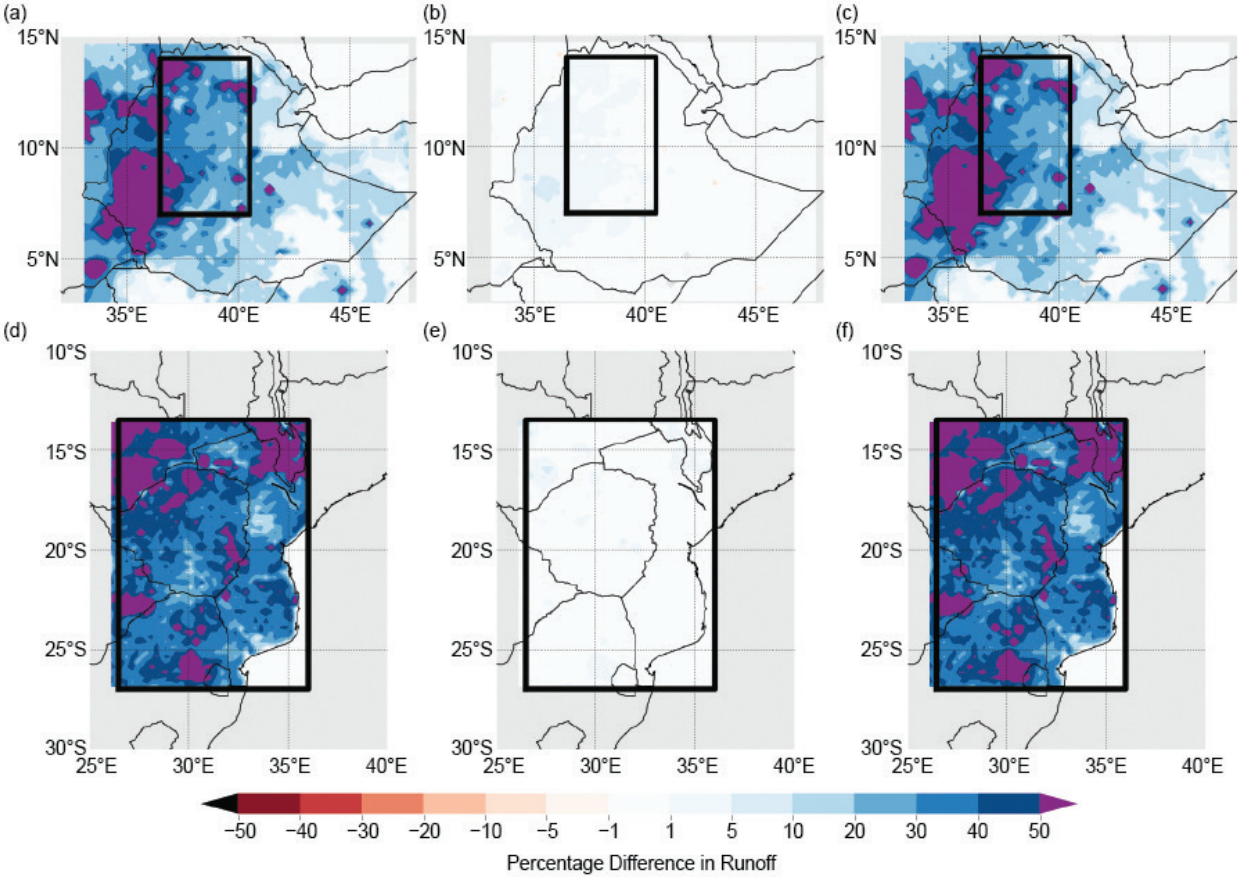

Fig. 15.2. Hydrologic sensitivity experiment results for runoff. (a),(d) The influence of anthropogenic rainfall reductions. (b),(e) The influence of local air temperature increases. (c),(f) Combines the effects of low rainfall and warm air temperatures. (a)–(c) NE experiments. (d)–(f) SA experiments. Each panel shows the change in runoff, in comparison with observed conditions, when rainfall and air temperatures are increased and/or cooled.

increase in eastern Pacific rainfall (Fig. 15.1d), one measure of the strength of ENSO (Chiodi and Harrison 2010; Chiodi and Harrison 2015; Curtis and Adler 2000). The magnitude of El Niño precipitation increases over the eastern Pacific would strongly influence El Niño's atmospheric forcing strength, and we find a precipitation decline (Fig. 15.1d) over southern Africa that is broadly consistent with our empirical analysis. Results from two other models and JJAS are similar (Supplemental Fig. S15.2).

Estimating Rainfall and Air Temperature Changes due to El Niño. Figures 15.1e,f show regressions between NE/SA rainfall and Niño-3.4 SSTs. Our study regions were chosen based on historical teleconnections (Supplemental Figs. S15.1e,f) and the pattern of the 2015–16 deficits. In Ethiopia and southern Africa, Niño-3.4 SSTs explained 45% and 53% of the 1981–82 to 2015–16 rainfall variance, respectively. While rainfall performance varied substantially during strong El Niños (the 1997–98 response was relatively modest in both regions), the observations suggest that a 1°C increase in El Niño-3.4 SSTs produces a 79 mm and 62 mm decrease in NE and SA rainfall, respectively. These regressions slopes suggest that without anthropogenic Niño-3.4 warming, NE and SA rainfall would have been approximately 16% and 24% greater, respectively.

ENSO teleconnections and warming trends were used to estimate anthropogenic air temperature changes of +0.9°C (Supplemental Material). Using the lower bounds of Niño-3.4 SST change (T_{JJAS}=0.6°C, T_{DJF}=0.7°C) gives estimates of a 9% and 14% rainfall change and a 0.8°C and 0.7°C JJAS/DJF air temperature change in NE and SA, respectively.

Contrapositive Hydrologic Experiment. We performed four hydrologic experiments using the variable infiltration capacity (VIC) model. In these experiments, we drove the VIC model with (i)

observed weather forcings, (ii) weather forcing in which we increased NE/SA precipitation by 16% and 24%, (iii) weather forcings with air temperatures cooled by +0.9°C/+0.9°C NE/SA, and (iv) weather forcings with both (i) and (ii) changes. Figure 15.2 shows results for experiments (ii)–(iv), expressed as anomalies from (i). Our contrapositive NE runoff changes, in our region of interest, for (ii)–(iv) were: +35%, +1%, +37%; for SA (ii)–(iv) changes were: +48%, +1%, +49%. Clearly, anthropogenic disruptions in precipitation, associated with the large increases in ENSO SST (Figs. 15.1a,b), provided the dominant contribution. As was the case for 2014 (Funk et al. 2015a), we find that a ~1°C warming over the tropical Pacific can have a much greater impact than a ~1°C warming in local air temperatures.

Conclusions. Anthropogenic warming contributed substantially to the very warm 2015/16 El Niño SSTs, and this anthropogenic contribution likely reduced NE and SA rainfall by approximately 16% and 24%. The associated simulated runoff reductions were much larger, 35% and 48%, respectively. A ~1°C warming over the tropical Pacific appears associated with a large (>70%) increase in El Niño diabatic forcing (Fig. 15.1f), and modest (~20%) precipitation reductions over NE/SA. These "modest" rainfall reductions, acting to accentuate natural El Niño impacts, have contributed to substantial food crises.

Recent El Niños appear to be more intense (Supplemental Fig. S15.2). During El Niños, warmer Indo-Pacific SSTs, and associated rainfall changes, may be more influential than the direct impacts of local increases in air temperatures. The contrast between Figs. 15.2a,b and 15.2d,e tell us that, based on these hydrologic simulations, nonlocal warming in the tropical Pacific had a much stronger drought impact than did relatively small local air temperature impacts. We feel this result is quite important, possibly indicating that a major mode of "climate change" may be associated with more extreme tropical SST and SST gradients. "Global warming" expressed as local increases in air temperatures may have less dramatic impacts. Assessments (Brown et al. 2015) of local temperature impacts on crop yields suggest relatively small yield reductions per degree of warming (~2% per °C). A degree of warming in Niño-3.4 SSTs, concomitant with a warm ENSO event, can have larger impacts due to teleconnected precipitation declines.

Because runoff forms a relatively small fraction of the hydrologic balance, the influence of rainfall deficits can be amplified, potentially leading to severe hydropower shortages (Davison 2015; Onishi 2016) and even severe drinking water deficits (Gauette 2016). These crises are just one aspect of the widespread food insecurity related to the extreme 2015/16 El Niño (Fig. 15.1), which is thought to have contributed to the severe food insecurity of 60 million people "primarily in the most vulnerable regions of southern Africa, East Africa, Central America, and the Pacific Islands" (OCHA 2016). If La Niña conditions follow, extreme warming in the western Pacific may lead to dry conditions over equatorial East Africa (Funk et al. 2015a; Funk et al. 2014; Shukla et al. 2014), exacerbating food insecurity conditions.

ACKNOWLEDGEMENTS. This research was supported by the US Geological Survey's Land Change Science program, the USAID Famine Early Warning Systems Network, and NASA SERVIR grant NNX16AM02G. Production of the rainfall data were supported by the USGS Earth Resources Observations and Science Center (http://earlywarning.usgs.gov/fews/datadownloads/Global/CHIRPS2.0). We would like to thank the Royal Netherlands Meteorological Institute for providing the CMIP5 simulations (https://climexp.knmi.nl) and the Earth System Research Laboratory Physical Sciences Division www.esrl.noaa.gov/) for providing the observed temperature and simulated precipitation fields.

REFERENCES

Brown, M., and Coauthors, 2015: *Climate Change, Global Food Security, and the U.S. Food System*. U.S. Department of Agriculture/U.S. Global Change Research Program, 146 pp., doi:10.7930/J0862DC7.

Camberlin, P., 1997: Rainfall anomalies in the source region of the Nile and their connection with the Indian summer monsoon. *J. Climate*, **10**, 1380–1392.

Chiodi, A. M., and D. E. Harrison, 2010: Characterizing warm-ENSO variability in the equatorial Pacific: An OLR perspective. *J. Climate*, **23**, 2428–2439, doi:10.1175/2009JCLI3030.1.

——, and ——, 2015: Global seasonal precipitation anomalies robustly associated with El Niño and La Niña events-An OLR perspective. *J. Climate*, **28**, 6133–6159, doi:10.1175/JCLI-D-14-00387.1.

Curtis, S., and R. Adler, 2000: ENSO indices based on patterns of satellite-derived precipitation. *J. Climate*, **13**, 2786–2793.

Davison, W., 2015: Ethiopia sees nationwide power cuts while drought dries dams. *Bloomberg News* [online], 1 December 2015. [Available online at www.bloomberg.com/news/articles/2015-12-01/ethiopia-sees-nationwide-power-cuts-while-drought-dries-dams.]

Degefu, W., 1987: Some aspects of meteorological drought in Ethiopia. *Drought and Hunger in Africa: Denying Famine a Future*, M. H. Glanz, Ed., Cambridge University Press, 23–36.

Diro, G., D. I. F. Grimes, and E. Black, 2011: Teleconnections between Ethiopian summer rainfall and sea surface temperature: Part II. Seasonal forecasting. *Climate Dyn.*, **37**, 121–131, doi:10.1007/s00382-010-0896-x.

FEWS NET, 2015: Illustrating the extent and severity of the 2015 drought, 7 pp.

——, 2016a: Food Security Outlook, Ethiopia: Large-scale food security emergency projected for 2016, 19 pp.

——, 2016b: Southern Africa Special Report: Illustrating the extent and severity of the 2015–2016 drought, 8 pp.

Funk, C., and Coauthors, 2005: Recent drought tendencies in Ethiopia and equatorial-subtropical eastern Africa. Vulnerability to Food Insecurity: Factor Identification and Characterization Rep. 01/2005, 12 pp. [Available online at http://pdf.usaid.gov/pdf_docs/PNADH997.pdf.]

——, M. D. Dettinger, J. C. Michaelsen, J. P. Verdin, M. E. Brown, M. Barlow, and A. Hoell, 2008: Warming of the Indian Ocean threatens eastern and southern African food security but could be mitigated by agricultural development. *Proc. Natl. Acad. Sci. USA*, **105**, 11081–11086, doi:10.1073/pnas.0708196105.

——, A. Hoell, S. Shukla, I. Bladé, B. Liebmann, J. B. Roberts, and G. Husak, 2014: Predicting East African spring droughts using Pacific and Indian Ocean sea surface temperature indices. *Hydrol. Earth Syst. Sci.*, **18**, 4965–4978, doi:10.5194/hess-18-4965-2014.

——, S. Shukla, A. Hoell, and B. Livneh, 2015a: Assessing the contributions of East African and west Pacific warming to the 2014 boreal spring East African drought [in "Explaining Extreme Events of 2014 from a Climate Perspective"]. *Bull. Amer. Meteor. Soc.*, **96 (12)**, S77–S81.

——, S. E. Nicholson, M. Landsfeld, D. Klotter, P. Peterson, and L. Harrison, 2015b: The Centennial Trends Greater Horn of Africa precipitation dataset. *Sci. Data*, **2**, 150050, doi:10.1038/sdata.2015.50.

——, and Coauthors, 2015c: The climate hazards infrared precipitation with stations–A new environmental record for monitoring extremes. *Sci. Data*, **2**, 150066, doi:10.1038/sdata.2015.66.

Gauette, N., 2016: U.S. dispatches emergency aid for Ethiopian drought. *CNN Politics, CNN* [online], 3 March 2016. [Available online at www.cnn.com/2016/03/03/politics/ethiopia-us-disaster-assistance-drought/index.html.]

Gissila, T., E. Black, D. Grimes, and J. Slingo, 2004: Seasonal forecasting of the Ethiopian summer rains. *Int. J. Climatol.*, 24, 1345–1358, doi:10.1002/joc.1078.

Hoell, A., C. Funk, T. Magadzire, J. Zinke, and G. Husak, 2015: El Niño–Southern Oscillation diversity and southern Africa teleconnections during austral summer. *Climate Dyn.*, **45**, 1583–1599, doi:10.1007/s00382-014-2414-z.

Huang, B., and Coauthors, 2015: Extended reconstructed sea surface temperature version 4 (ERSST. v4). Part I: Upgrades and intercomparisons. *J. Climate*, **28**, 911–930, doi:10.1175/JCLI-D-14-00006.1.

Jury, M. R., and C. Funk, 2013: Climatic trends over Ethiopia: Regional signals and drivers. *Int. J. Climatol.*, **33**, 1924–1935, doi:10.1002/joc.3560.

——, C. Mc Queen, and K. Levey, 1994: SOI and QBO signals in the African region. *Theor. Appl. Climatol.*, **50**, 103–115.

Korecha, D., and A. G. Barnston, 2007: predictability of June-September rainfall in Ethiopia. *Mon. Wea. Rev.*, **135**, 628–650, doi:10.1175/MWR3304.1.

——, and A. Sorteberg, 2013: Validation of operational seasonal rainfall forecast in Ethiopia. *Water Resour. Res.*, **49**, 7681–7697, doi:10.1002/2013WR013760.

Lindesay, J., 1988: South African rainfall, the Southern Oscillation and a Southern Hemisphere semi-annual cycle. *Int. J. Climatol.*, **8**, 17–30, doi:10.1002/joc.3370080103.

Misra, V., 2003: The influence of Pacific SST variability on the precipitation over Southern Africa. *J. Climate*, **16**, 2408–2418, doi:10.1175/2785.1.

Nicholson, S. E., and M. D. Entekhabi, 1986: The quasi-periodic behavior of rainfall variability in Africa and its relationship to the Southern Oscillation. *Arch. Meteor. Geophys. Bioclimatol., Ser. A*, **34**, 311–348.

——, and J. Kim, 1997: The relationship of the El Nino–Southern oscillation to African rainfall. *Int. J. Climatol.*, **17**, 117–135.

OCHA, 2016: El Nino: Overview of impact, projected humanitarian needs and response. U.N. Office for the Coordination of Humanitarian Affairs, 20 pp. [Available online at https://docs.unocha.org/sites/dms/Documents/OCHA_ElNino_Overview_13Apr2016.pdf.]

Onishi, N., 2016: Climate change hits hard in Zambia, an African success story. *New York Times* [online], 12 April 2016. [Available online at www.nytimes.com/2016/04/13/world/africa/zambia-drought-climate-change-economy.html?_r=0.]

Reason, C., R. Allan, J. Lindesay, and T. Ansell, 2000: ENSO and climatic signals across the Indian Ocean basin in the global context: Part I, Interannual composite patterns. *Int. J. Climatol.*, **20**, 1285–1327.

Rocha, A., and I. Simmonds, 1997: Interannual variability of south-eastern African summer rainfall. Part I: Relationships with air-sea interaction processes. *Int. J. Climatol.*, **17**, 235–265.

Segele, Z. T., and P. J. Lamb, 2005: Characterization and variability of Kiremt rainy season over Ethiopia. *Meteor. Atmos. Phys.*, **89**, 153–180, doi:10.1007/s00703-005-0127-x.

Shukla, S., C. Funk, and A. Hoell, 2014: Using constructed analogs to improve the skill of March-April-May precipitation forecasts in equatorial East Africa. *Environ. Res. Lett.*, **9**, 094009, doi:10.1088/1748-9326/9/9/094009.

Viste, E., D. Korecha, and A. Sorteberg, 2012: Recent drought and precipitation tendencies in Ethiopia. *Theor. Appl. Climatol.*, **112**, 535–551, doi:10.1007/s00704-012-0746-3.

Williams, A. P., and Coauthors, 2012: Recent summer precipitation trends in the Greater Horn of Africa and the emerging role of Indian Ocean sea surface temperature. *Climate Dyn.*, **39**, 2307–2328, doi:10.1007/s00382-011-1222-y.

Wittenberg, A. T., 2009: Are historical records sufficient to constrain ENSO simulations? *Geophys. Res. Lett.*, **36**, L12702, doi:10.1029/2009GL038710.

Table 28.1. Summary of Results

	ANTHROPOGENIC INFLUENCE ON EVENT		
	INCREASE	**DECREASE**	**NOT FOUND OR UNCERTAIN**
Heat	**Global Temperature** (Ch. 2) **South India & Sri Lanka** (Ch. 2) **Central Europe** (Ch. 11) **Europe** (Ch. 12) **Ethiopia and Southern Africa** (Ch. 15) **N.W. China** (Ch. 19) **W. China** (Ch. 20) **Japan** (Ch. 21) **Indonesia** (Ch. 22) **S. Australia** (Ch. 23) **Australia** (Ch. 24)		**Central Equitorial Pacific** (Ch. 2)
Cold		**Northeastern U.S.** (Ch. 7)	**Mid-South Atlantic U.S.** (Ch. 7) **N. America** (Ch. 8)
Heat & Humidity	**Egypt** (Ch. 14) **India & Pakistan** (Ch. 16)		
Dryness	**Indonesia** (Ch. 22) **Tasmania** (Ch. 25)		
Heavy Precipitation	**China** (Ch. 18)		**Nigeria** (Ch. 13) **India** (Ch. 17)
Sunshine	**United Kingdom** (Ch. 10)		
Drought	**Canada** (Ch. 9) **Ethiopia and Southern Africa** (Ch. 15)		
Tropical Cyclones	**Western North Pacific** (Ch. 26)		
Wildfires	**Alaska** (Ch. 4)		
Sea Ice Extent		**Arctic** (Ch. 27)	
High Tide Floods	**Southeastern U.S.** (Ch. 6)		
Snowpack Drought	**Washington U.S.** (Ch. 5)		
TOTAL	**23**	**2**	**5**

	METHOD USED	Total Events
Heat	Ch. 2: **CMIP5 modeling** Ch. 11: **Observations; weather@home modeling** Ch. 12: **HadGEM3-A modeling** Ch. 15: **CMIP5 modeling** Ch. 19: **CMIP5 modeling with ROF; FAR** Ch. 20: **CMIP5 modeling with ROF; FAR** Ch. 21: **MIROC5-AGCM modeling** Ch. 22: **Observations; CMIP5 modeling** Ch. 23: **weather@home modeling; FAR** Ch. 24: **BoM seasonal forecast attribution system and seasonal forecasts**	12
Cold	Ch. 7: **Observations; CMIP5 modeling** Ch. 8: **AMIP (IFS model) modeling**	3
Heat & Humidity	Ch. 14: **weather@home modeling** Ch. 16: **Non-stationary EV theory; C20C+ Attribution Subproject**	2
Dryness	Ch. 22: **Observations; CMIP5 modeling** Ch. 25: **Observations; Modeling with CMIP5 and weather@home**	2
Heavy Precipitation	Ch. 13: **Observations; Modeling with CAM5.1 and MIROC5** Ch. 17: **Observations; Modeling with weather@home, EC-Earth and CMIP5** Ch. 18: **HadGEM3-A-N216 modeling; FAR**	3
Sunshine	Ch. 10: **Hadley Centre event attribution system built on the high-resolution version of HadGEM3-A**	1
Drought	Ch. 9: **Observations; CMIP5 modeling; Trend and FAR analyses** Ch. 15: **CMIP5 modeling, land surface model simulations, and statistical analyses**	2
Tropical Cyclones	Ch. 26: **GFDL FLOR modeling; FAR**	1
Wildfires	Ch. 4: **WRF-ARW optimized for Alaska with metric of fire risk (BUI) to calculate FAR**	1
Sea Ice Extent	Ch. 27: **OGCM modeling**	1
High Tide Floods	Ch. 6: **Tide-gauge data; Time-dependent EV statistical model**	1
Snowpack Drought	Ch. 5: **Observations; CESM1 modeling**	1
		30

ACRONYMS:

AMIP: Atmospheric Model Intercomparison Project
BoM: Bureau of Meteorology, Australia
BUI: Buildup Index
CAM: Community Atmosphere Model, http:www.cesm.ucar.edu
CESM: Community Earth System Model
CMIP: Coupled Model Intercomparison Project
FAR: Fraction of Attributable Risk
EC-EARTH: https://verc.enes.org/
EV: Extreme Value
GFDL FLOR: Geophysical Fluid Dynamics Laboratory Forecast version Low Ocean Resolution
GHCN: Global Historical Climatology Network
IFS: Integrated Forecast System
MIROC5–AGCM: Model for Interdisciplinary Research on Climate–Atmospheric General Circulation Model
OGCM: Ocean General Circulation Model
ROF: Regularized Optimal Fingerprinting
weather@home: http:www.climateprediction.net/weatherathome
WRF-ARW: Advanced Research (ARW) version of the Weather Research and Forecasting (WRF) model